

# INTERACTION OF A TRANSONIC DISLOCATION WITH DEFECTS

S. Q. SHI, W. J. ZHU, C. H. WOO AND H. HUANG

*Department of Mechanical Engineering  
The Hong Kong Polytechnic University, Hong Kong*

## ABSTRACT

During deformation of crystalline solids at ultra-high strain rates, supersonic dislocations may be generated, which has been demonstrated in molecular dynamics simulation. These supersonic dislocations may encounter various kinds of defects in a solid, and may be slowed, or even pinned. In this work, we use the molecular dynamics method to study the dynamics of transonic dislocations during their interactions with a subsonic dislocation, a small void, or a small interstitial loop. The results indicate that a subsonic dislocation right in front of transonic dislocation will slow it down below the speed of sound. However, small defects, like voids and interstitial clusters, will only temporarily hold up a segment of the transonic dislocation. Upon release from the clusters, this segment of dislocation was re-accelerated to become transonic again. The interstitial loop has a much stronger pinning effect on the moving dislocation as compared to a void. The moving edge dislocation absorbed the interstitial loop by forming jogs, while it swept the void into a few smaller defects of vacancy type.

## 1. INTRODUCTION

Dislocations play the pivotal role in mechanical deformation of crystalline solids. In general, the dislocations move with velocities that increase with the deformation rate. According to the linear elasticity theory, a dislocation cannot be accelerated beyond the transverse speed ( $c_t$ ) of sound in solids. However, recent molecular dynamics simulations indicate that a transonic (i.e., with a velocity higher than  $c_t$  but lower than longitudinal speed of sound,  $c_l$ ), or even supersonic dislocation (i.e., with a velocity is higher than  $c_l$ ) can be produced, if the solid is subjected to a sufficiently high deformation rate [1-3].

The interaction of dislocations with other defects in the solid, such as various boundaries, other dislocations, point defects and their clusters, are important topics of investigation in the theory of dislocations and crystalline plasticity. The possibility of transonic and supersonic dislocations raises the natural question of how will this new species behave in the presence of these other defects. Indeed, the theory of dislocations will be left incomplete without such knowledge. This paper reviews our recent work in this area.

In Section 2, we will present the simulation method, followed by details of the simulation results in Section 3. Finally, we summarize the conclusions in Section 4.

## 2. SIMULATION METHOD

In our simulation, we consider the practically elastically isotropic material tungsten, for which the continuum linear elasticity theory provides the best description. The inter-atomic interaction is described by the many-body Finnis-Sinclair potential [4, 5]. A block of tungsten crystal containing more than half a million atoms was arranged as in Figure 1. To create natural edge dislocations in the body-centered cubic lattice of tungsten,  $\langle 111 \rangle$  direction was aligned with the x-axis (horizontal direction),  $\langle 2\bar{1}\bar{1} \rangle$  with the y-axis (vertical direction), and  $\langle 0\bar{1}\bar{1} \rangle$  with the z-axis (transverse direction). The bottom edge of the block was held fixed, and the top edge of the block was allowed to move only horizontally. Periodic boundary condition was applied in z direction. Both surfaces in the y-direction were free, except for the left upper half, which was pushed to the right at a constant velocity to simulate an indentation process. This process efficiently create edge dislocations with Burgers vector  $\mathbf{b} = a_0/2 \langle 111 \rangle$  at the sharp edge of the indentation.

The indentation was applied in the anti-twinning direction, and the motions of all atoms were followed in the MD simulation at sufficiently small time steps between 1 ~ 10 fs ( $10^{-15} \sim 10^{-14}$  second), to ensure stable and consistent results. The simulations were started at a low temperature of 10 K, and at an indentation speed of 75 m/s. Under this condition, a transonic dislocation is generated on the center plane (i.e., the  $y = 0$  plane).

We have studied the interaction of a transonic dislocation with a subsonic dislocation, a small void, and an interstitial cluster, one at a time. The subsonic dislocation is initially introduced as a dipole by removing a column of atoms. The negative dislocation is sucked out to the free surface, leaving inside only the positive part of the dipole on the same glide plane as the transonic dislocation – which is also positive. The small void is created by removing a cluster of atoms centered on the glide plane of the transonic dislocation. Similarly, a self-interstitial dislocation loop is created by adding a cluster of interstitial atoms on the glide plane of the transonic dislocation.

In this report, location is described in terms of the number of inter-atomic spacings from the origin of the coordinates (0,0,0). And this origin of the coordinates is located at the centre of the crystal. Note that the inter-atomic spacings are different in the three directions. For example, in x-direction (i.e.,  $\langle 111 \rangle$ ), the inter-atomic spacing is the Burgers vector,  $b$ . To describe the location in real space, the current coordinates have to be multiplied by the nearest neighbor distance in the direction concerned.

## 3. SIMULATION RESULTS

### 3.1 Transonic dislocation with a small void

A small void containing 11 atoms was “cut” out from the crystal at the location around (5,0,0). After a short relaxation, the indentation process was started. Three consecutive transonic dislocations were generated. The first dislocation readily cut through and sheared the void. The 2<sup>nd</sup> and 3<sup>rd</sup> dislocations then swept up the top half of the void and re-deposited it in four smaller defect clusters, each containing one or two vacancies.

The location of dislocations at time intervals of 400 fs were recorded and plotted as a function of time in Figure 2. The straight lines in this figure are fitting lines to the data before

dislocations reached the void. One can see clearly that the velocity of each dislocation was constant before reaching the void. At the time when they cut through the small void, the velocity for the center portion of the dislocations was slowed down. In some cases, the velocity was reduced to below  $c_t$  for a short period of time, then accelerated to transonic or even supersonic velocity. In the supersonic case (the 3<sup>rd</sup> dislocation), this dislocation was approaching the free surface. This may be the first evidence that a curved dislocation can travel from subsonic speed up to transonic speed and higher and overcome the traditional sound barrier  $c_t$ .

### 3.2 Transonic dislocation with a subsonic dislocation

After removing a column of atoms, the indentation process was started. The vacancy plane collapsed to form a dislocation dipole – a positive edge dislocation formed with the same glide plane as the transonic dislocations and a negative edge dislocation formed at a few atomic distances below. Under the high shear stress, the positive dislocation accelerated very fast to about 2.06 km/s (about  $0.74c_t$ ) and maintained at this speed (see Figure 3), while the negative dislocation moved to the left and disappeared on the surface. It seems that this  $0.74c_t$  is apparently a stable state of subsonic dislocations, as can also be seen in [1]. Note that the Rayleigh wave has a speed of about  $0.9c_t$  [6] in tungsten. The reason for this value of  $0.74c_t$  is still not clear. As the indentation continued, a transonic dislocation was created and moved at a fairly constant speed of 4.14 km/s (about  $1.48c_t$ ), see Figure 3. This is close to the radiation-free state of a moving dislocation found by Eshelby [7]. When the transonic dislocation caught up with the subsonic one, the two dislocations maintained a close distance of  $5\sim 7b$  between them, and moved together with subsonic velocity afterwards. From Fig.3 it is quite clear that the transonic dislocation did not change much of its speed until it reached the minimum distance from the subsonic dislocation, neither did the subsonic dislocation. This is consistent with the classical theory prediction that the stress field of high velocity dislocations is contracted in the moving direction. At the moment when the transonic dislocation reached the minimum distance with the subsonic one, the subsonic dislocation was seen to accelerate momentarily over  $c_t$ , as if it was “kicked” by the transonic dislocation. This may be an indication that a straight dislocation may overcome the traditional sound barrier  $c_t$ .

### 3.3 Transonic dislocation with a self-interstitial loop

The atomic arrangement of the (112) plane in BCC is characterized by six types of geometrical stacking sequence. To create a SIL on the glide plane of the edge dislocation, two adjacent types of atomic planes are inserted on ( $\bar{2}11$ ) plane just above the  $y = 0$  plane. After the insertion, the crystal was allowed to relax by quenching and annealing, and finally stabilization at 10 K. The diameter of the SIL is about 2.5 nm, (top view in Figure 4) on the x-z plane at  $y = 0$ . Inside the loop, there is a stacking fault. Brighter color always indicates higher potential energy of the atoms. From Figure 5 (view on plane  $z = 0$ ), one can see that it is a sessile, self-interstitial loop with Burgers vectors  $\mathbf{b} = a_o\langle 100 \rangle$  on the left side (loop ABCDE), and  $a_o\langle \bar{1}00 \rangle$  on the right side (loop DCFHJ). The overall displacement is zero (loop ABCFHJA).

Once the SIL has settled down, the indentation process starts. The time step in this simulation was 1 fs. The temperature of the crystal increased to less than 40K during the indentation.

When the first edge dislocation intersects the SIL, the center part of the edge dislocation was trapped by the SIL. Figure 6 presents some snapshots on the plane of  $z = 0$ . The interaction between the gliding edge dislocation and SIL favors a displacement along the  $[\bar{1}11]$  direction, based on a simple geometry and energy analysis. Indeed, one can see that the displacement on the right hand side of the SIL changed to  $a_o/2\langle\bar{1}11\rangle$ , while the displacement on the left hand side of the SIL remained the same  $a_o\langle 100\rangle$ , Figure 6(7). The overall displacement is  $a_o/2\langle 111\rangle$ , as it should be. At the next snapshot, Figure 6(8), a vacancy appeared which may come from the core of original SIL.

As the deformation continued, an area with high strain energy developed to the right side of the SIL, see Figures 6(9) and (10). And suddenly a shear zone was created at about 3 atomic planes below the glide plane of the original edge dislocation, Figures 6(11) and (12). When this happened, the overall displacement around the location of the original SIL became  $a_o\langle 100\rangle$ , that is, the displacement of  $a_o/2\langle\bar{1}11\rangle$  at the right hand side of the SIL disappeared, see Figure 6(12). This shear zone may be viewed as a widened edge dislocation core that spreads over more than 10 atomic distances, and a moment later it quickly converged into a normal edge dislocation of  $a_o/2\langle 111\rangle$  moving to the right, (Figures 6(13) and (14)). As a result, the originally straight edge dislocation now becomes jogged at the center part, see a projected view in the  $\langle\bar{1}\bar{1}\bar{1}\rangle$  direction of the dislocation in Figure 7. This view reveals that this center part of the dislocation was gliding on the  $(\bar{1}10)$  and  $(\bar{1}01)$  planes with the same Burgers vector,  $a_o/2\langle 111\rangle$ .

The second edge dislocation entered the “SIL” in Figure 6(13) (the double quote means that this was not the original SIL). By the time of Figure 6(15), the configuration of the displacement became the same as in Figure 6(8), that is, left side  $a_o\langle 100\rangle$  and right side  $a_o/2\langle\bar{1}11\rangle$ , except for an extra vacancy cluster (both are visible in Figure 6(15)). The following deformation process was similar to that for the first edge dislocation, except that, at this time, the two displacements at “SIL” annihilate each other and formed a perfect edge dislocation  $a_o/2\langle 111\rangle$  at a plane 3 atomic distance below the original gliding plane, Figure 6(19). At this point, the “SIL” disappeared, and all the interstitial atoms within the SIL have carried along by two edge dislocations in the form of jogged planes. As a result, there is no more trapping effect on the third edge dislocation.

The locations of edge dislocations as a function of time are given in Table 1. And because of the interaction within the SIL, it is difficult to determine the location around the SIL and “SIL”. Therefore, a “N/A” for “not available” is given for these cases. Top views corresponding to Figure 6 are given in Figure 8. It is clear that the center part of the dislocations was trapped by the SIL and by “SIL”. The two tilted planes formed after intersect were on the planes  $(\bar{1}10)$  and  $(\bar{1}01)$ , respectively. It may be interesting to note that the jogged part has an initial velocity higher than the sound barrier  $c_t$ .

#### 4. CONCLUSIONS

Interactions between transonic edge dislocation and void or subsonic edge dislocation or self-interstitial loop were studied in this report using MD method. It was found in this highly non-linear regime that

- Part of a curved dislocation can move across the traditional sound barrier from transonic to subsonic and vice versa during the interaction with a void;
- Vacancy type of defects can move with dislocation at very high speed, at least for a short period of time, then condense into a few smaller defects of vacancy type;
- A velocity of  $0.74c_t$  is apparently a stable speed for subsonic edge dislocation under high shear stress;
- Also at high shear stress, the transonic edge dislocation intends to move at about the radiation-free state of a moving dislocation discovered by Eshelby;
- The transonic edge dislocation may be slowed down by a subsonic edge dislocation gliding on the same plane; and the subsonic dislocation may be “pushed” across the sound barrier by the transonic one; And thus the conclusion about sound barrier made from linear elastic theory is seen to be invalid in this regime;
- A minimum distance may exist between two edge dislocations under high shear stress;
- The SIL has a stronger pinning effect on transonic dislocations, as compared to a void;
- The SIL can be annihilated by being carried along with the transonic dislocations in the form of jogs.

#### ACKNOWLEDGEMENT

The work described in this paper was supported by central research grants from the Hong Kong PolyU (G-T090 and G-T286), and by a grant from the Research Grants Council of the Hong Kong Special Administrative Region (PolyU1/99C).

#### REFERENCES

- [1] P. Gumbsch and H. Gao, *Science*, vol.283, p.965 (1999).
- [2] S.Q. Shi, H. Huang and C.H. Woo, *Comp. Mater. Sci.*, in press.
- [3] S.Q. Shi, W.J. Zhu, H. Huang, C.H. Woo, *Rad. Defects in Solids*, submitted.
- [4] M.W. Finnis and J.E. Sinclair, *Philos. Mag. A*, vol.50, p.45 (1984).
- [5] G.J. Ackland and R. Thetford, *Philos. Mag. A*, vol.56, p.15 (1987).
- [6] J.P. Hirth and J. Lothe, *Theory of Dislocations*, Wiley, New York, (1982).
- [7] J.D. Eshelby, *Proc. Phys. Soc.*, vol.62A, p.307 (1949).

Table 1. Locations and velocities\* of dislocations at central plane ( $z = 0$ )

Time ( $10^{-13}$ s)	1 <sup>st</sup> dislocation		2 <sup>nd</sup> dislocation		3 <sup>rd</sup> dislocation	
	Location (x)	Velocity (km/s)	Location (x)	Velocity (km/s)	Location (x)	Velocity (km/s)
100	-29.5					
105	-23.2	3.45				
110	-17.5	3.12				
115	-9.8	4.22				
120	-3.7	3.34				
125	3.3	3.84				
130	7.3	2.19				
135	13	3.12				
140	13	0				
145	13	0				
150	13	0	-28			
155	13	0	-23	2.74		
160	13	0	-14.5	4.66		
165	21	4.38	-7.3	3.95		
170	27	3.29	-0.5	3.73		
175	31.2	2.3	7.5	4.38		
180	40	4.82	12	2.45		
185			14	1.1	-32.0	
190			14	0	-26.0	3.29
195			14	0	-21	2.74
200			20.5	3.56	-12.5	4.66
205			26	3.02	-5.0	4.11
210			34.8	4.82	2.0	3.84
215			40	2.85	9.0	3.84
220					13.0	2.19
225					22.0	4.93
230					28.0	3.29
235					32.0	2.19
240					33.0	0.55
245					35.0	1.10

\*Velocities were calculated using the data from current moment and one time step earlier.

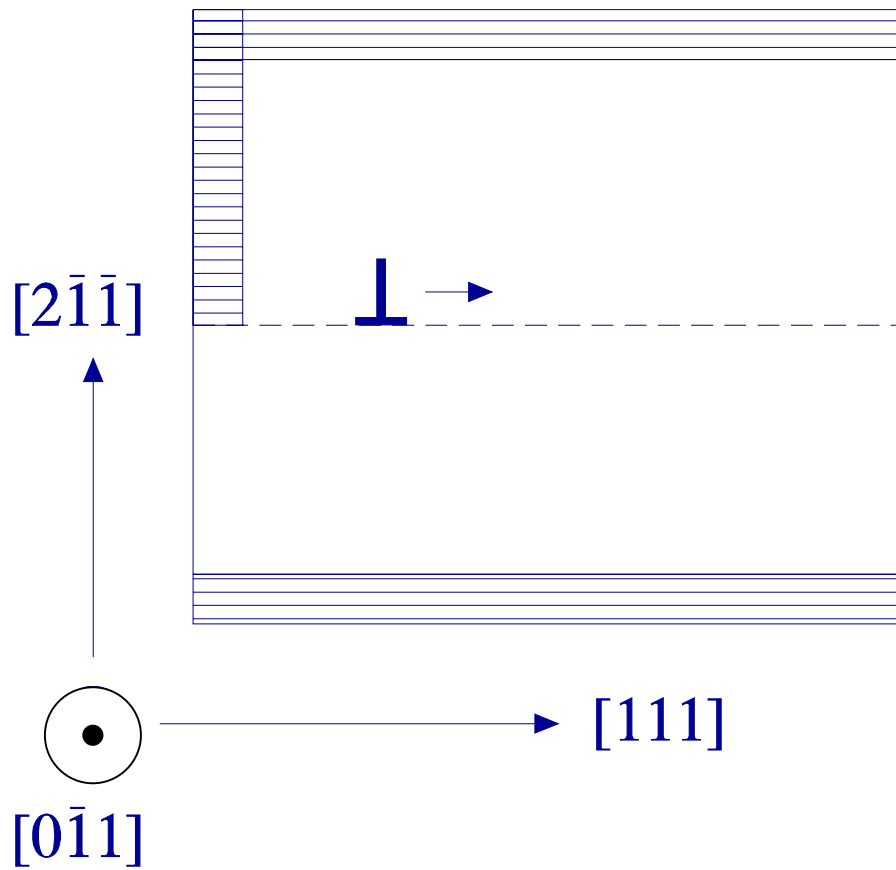


Figure 1. Schematic plot of crystal orientation of tungsten in MD simulation.

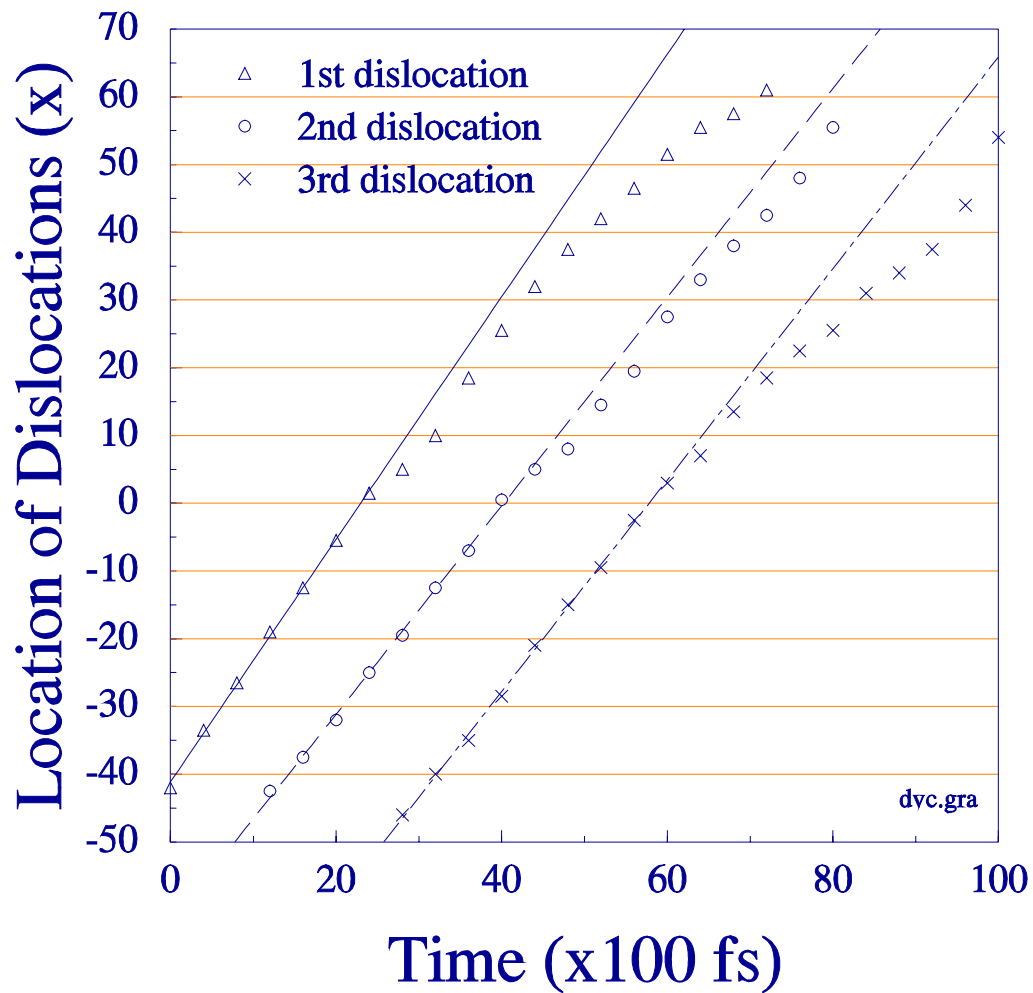


Figure 2. The locations of dislocations on the plane  $z = 0$ . Straight lines were obtained by fitting to the early parts of data.

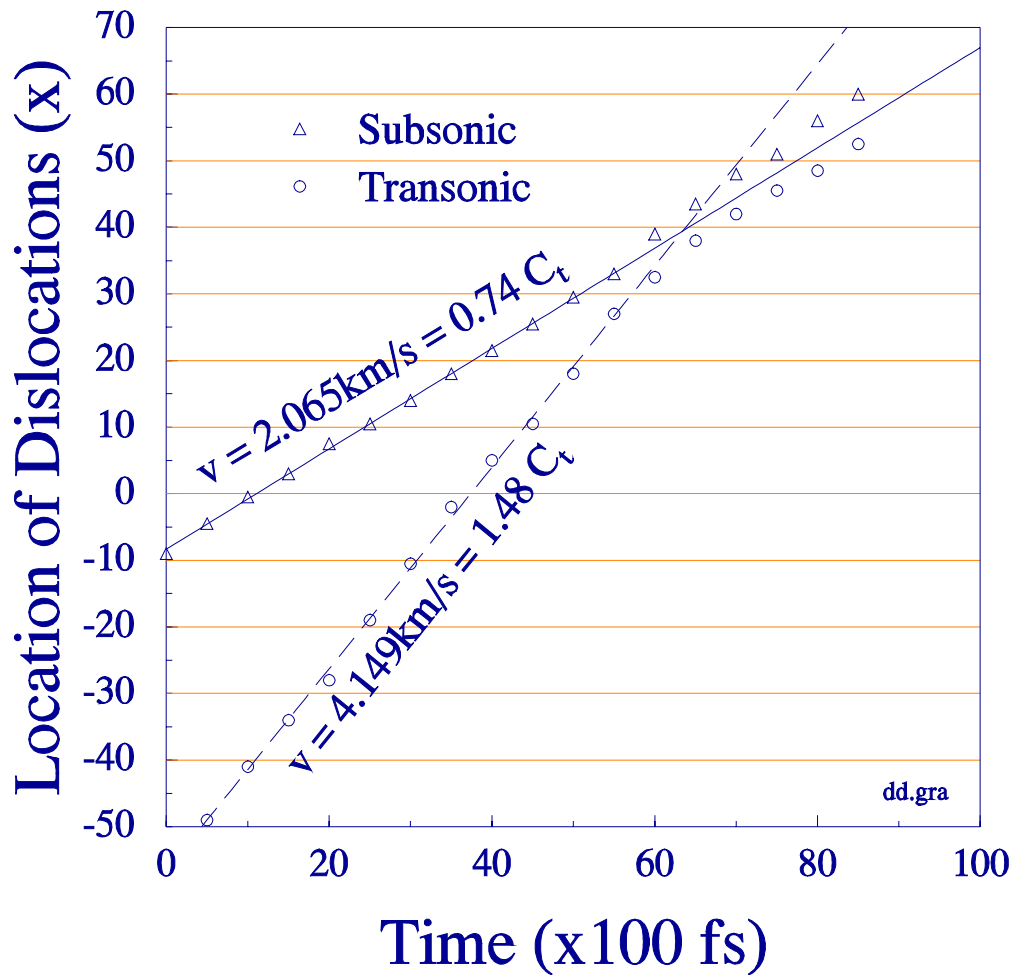


Figure 3. The locations of a transonic dislocation and a subsonic dislocation on the plane  $z = 0$  as a function of time. Straight lines were obtained by fitting to the data up to 5500 femto seconds.

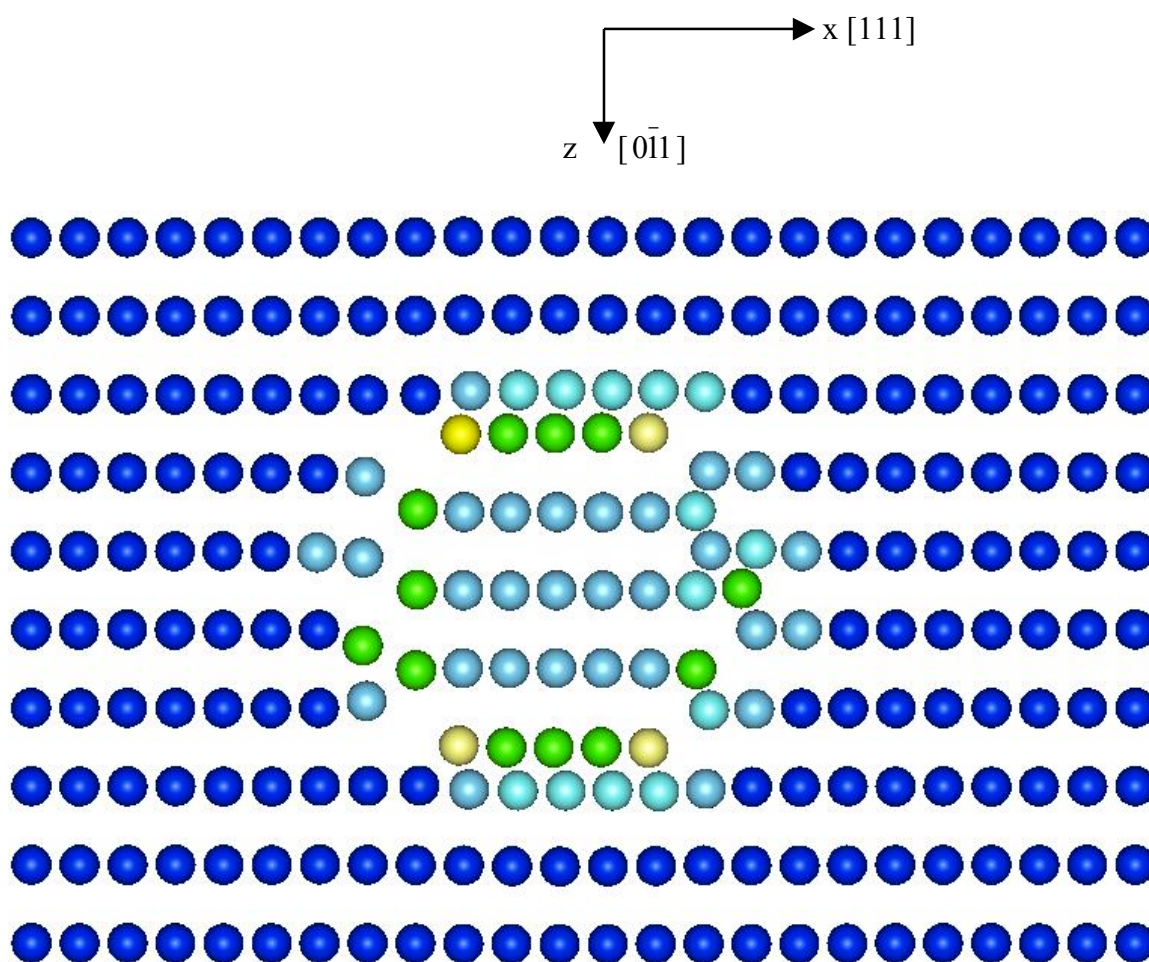


Figure 4. Top view of SIL on the plane of  $y = 0$ .

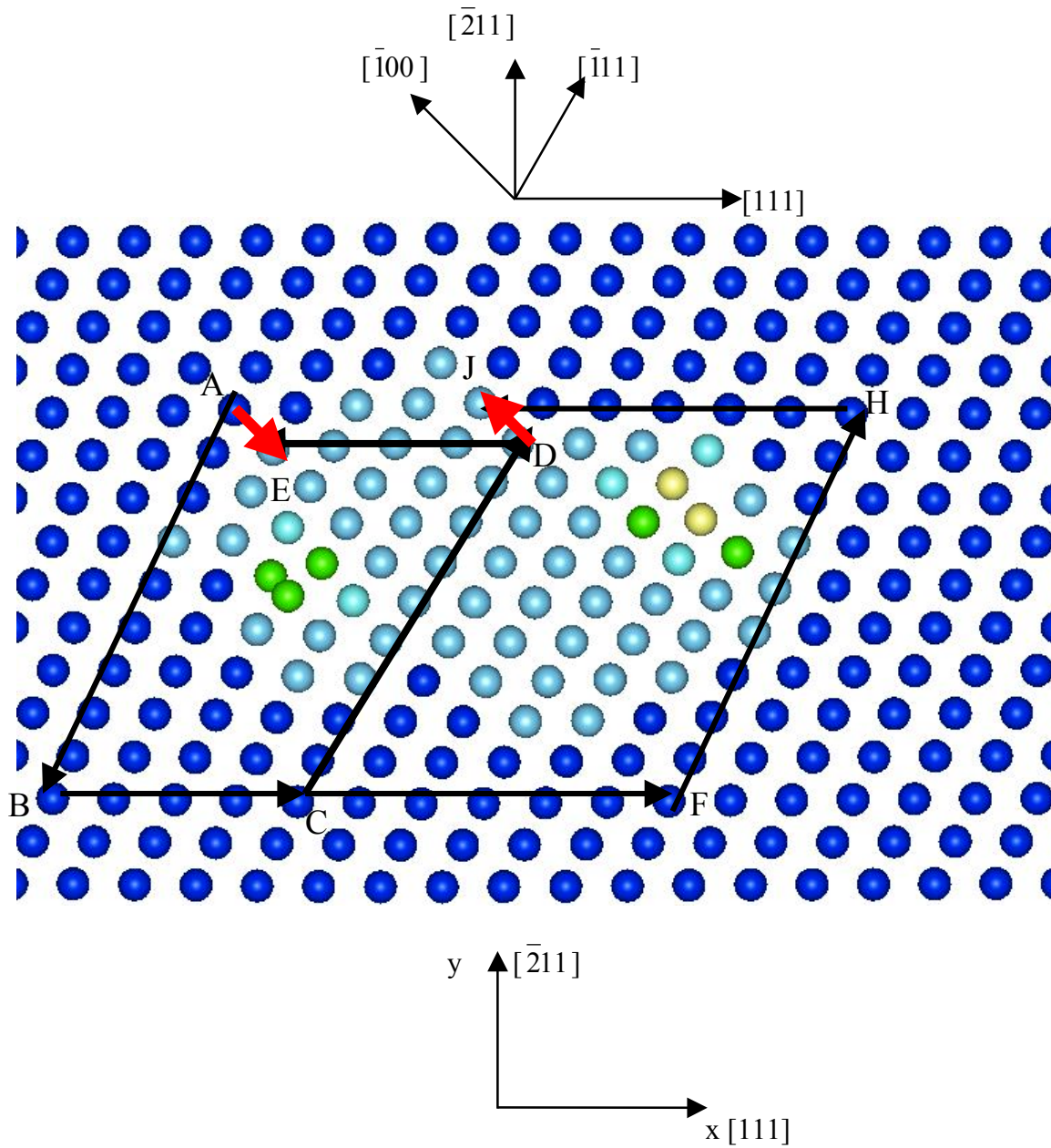
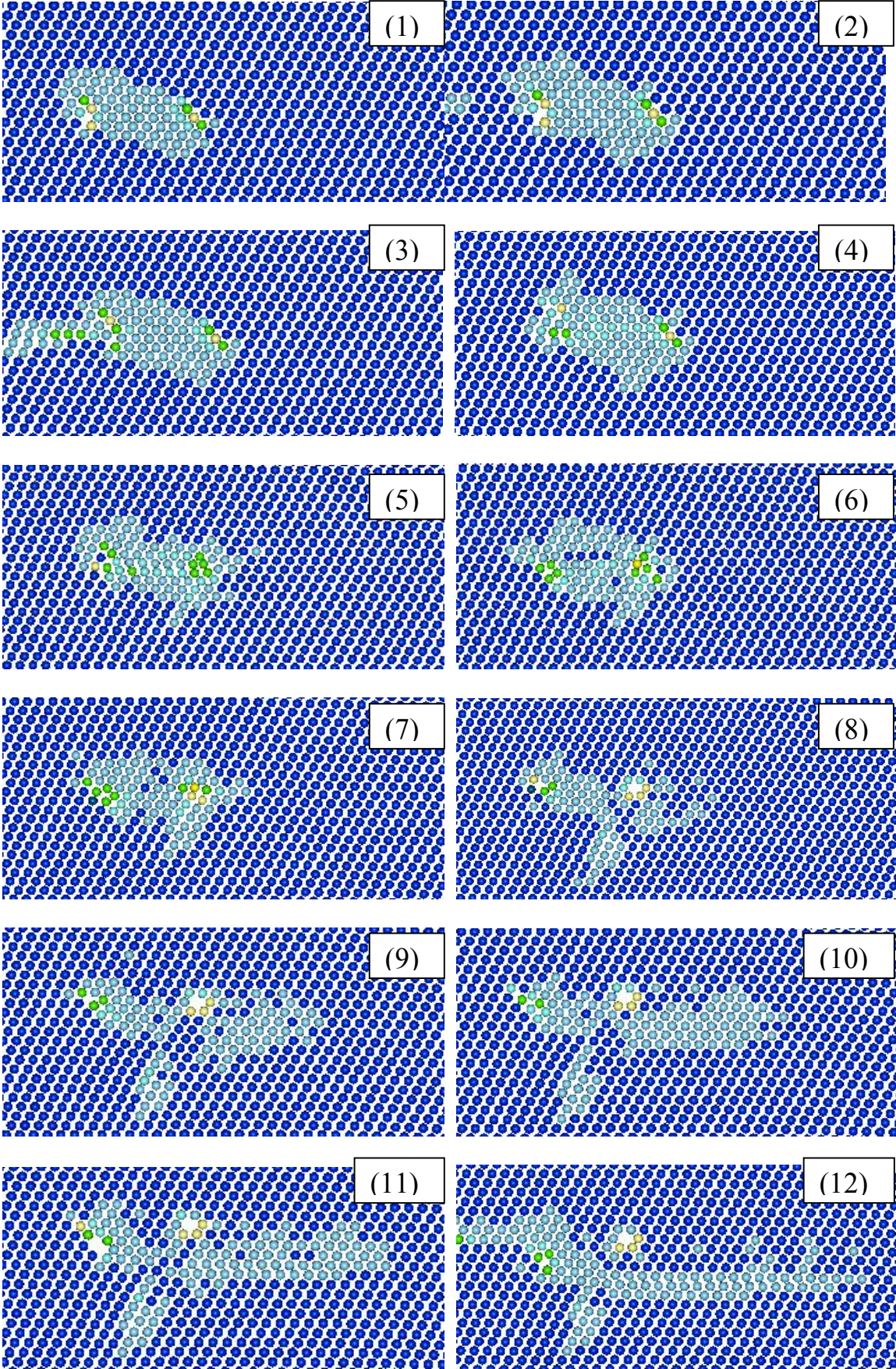


Figure 5. Front view of SIL on the plane of  $z = 0$ .



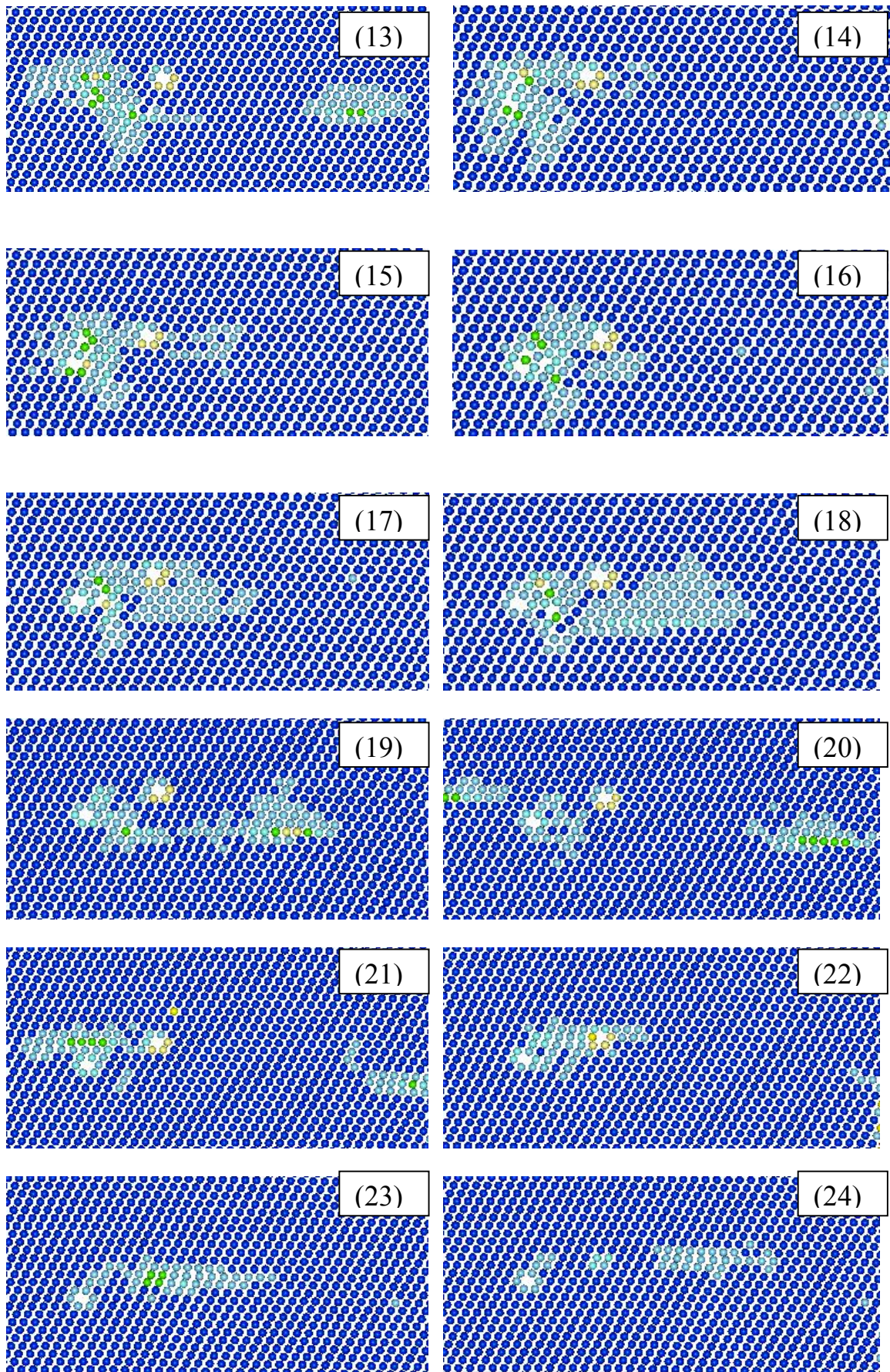


Figure 6. Snapshots of front view on the plane of  $z = 0$ .

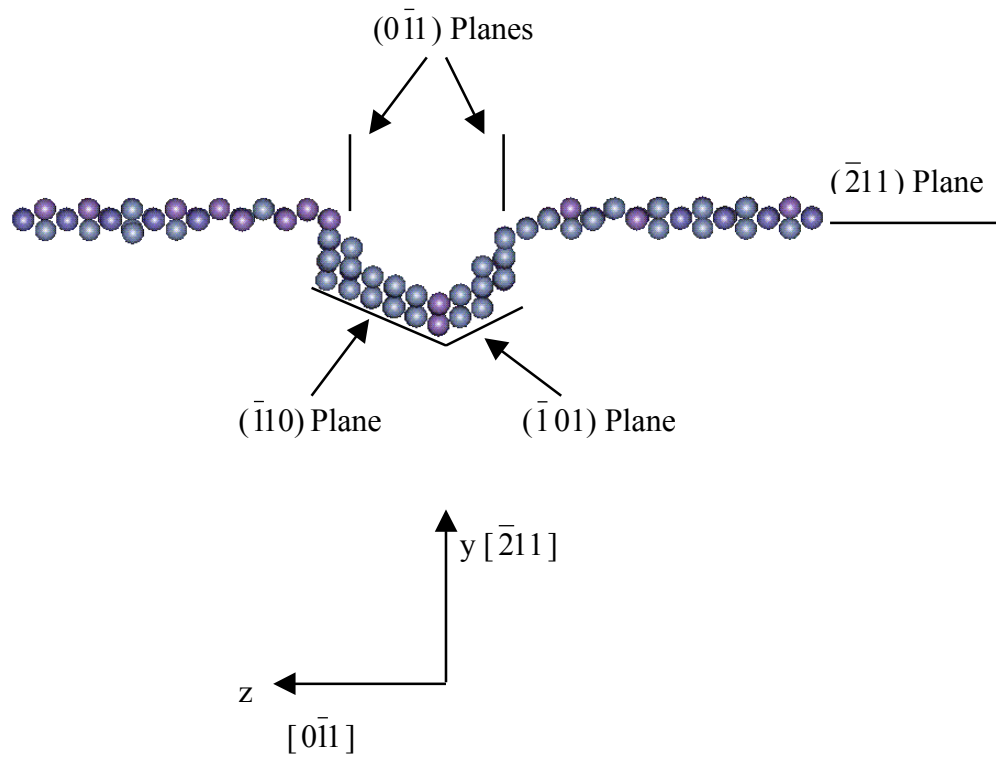
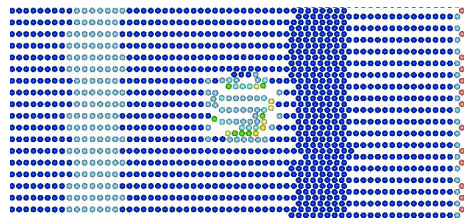
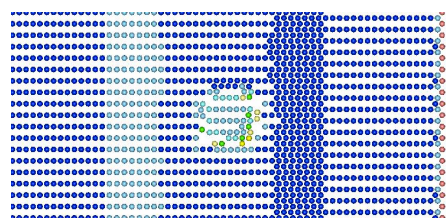


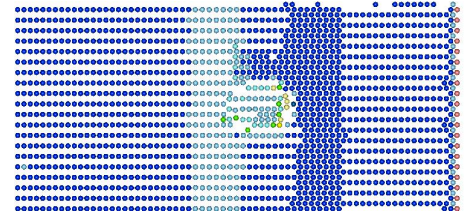
Figure 7. The projected view in the  $[\bar{1}\bar{1}\bar{1}]$  direction of the moving edge dislocation. Only atoms with high energy at the dislocation core are shown. The center part (jogs) is moving a few atomic planes below the original  $(\bar{2}11)$  plane and dragged behind the two side wings in the  $[\bar{1}\bar{1}\bar{1}]$  direction.



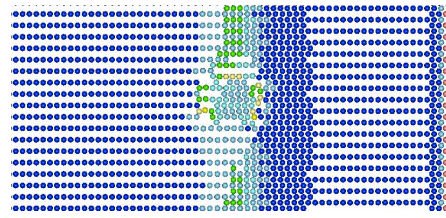
(1)



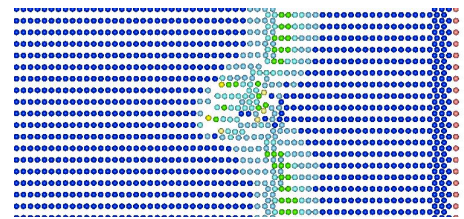
(2)



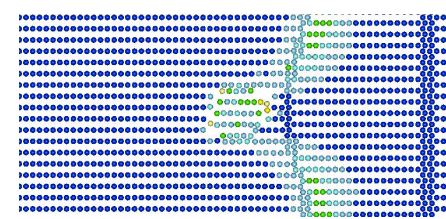
(3)



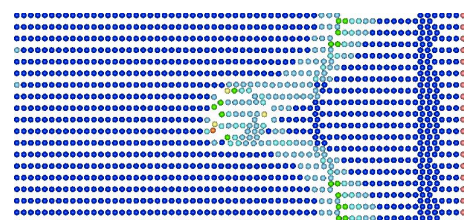
(4)



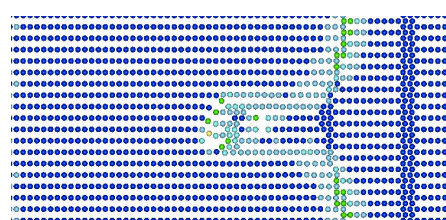
(5)



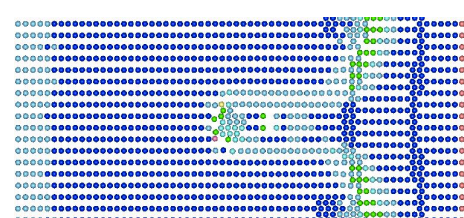
(6)



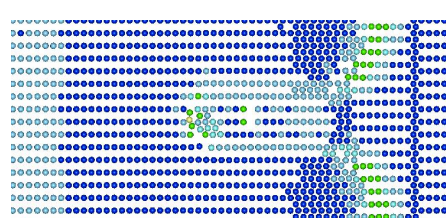
(7)



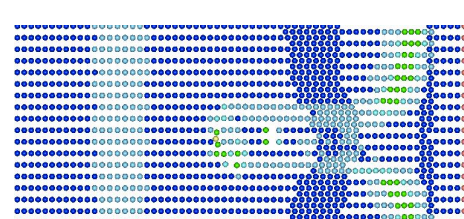
(8)



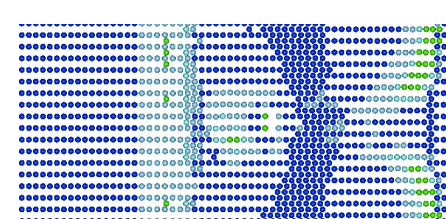
(9)



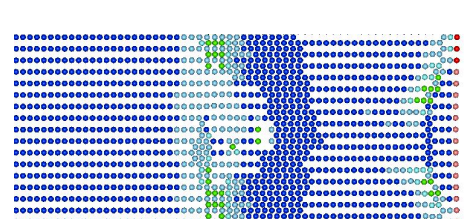
(10)



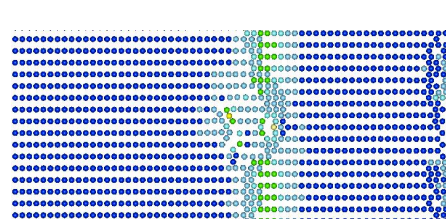
(11)



(12)



(13)



(14)

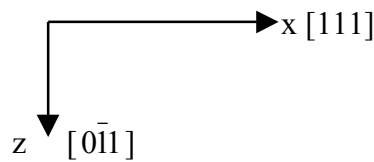
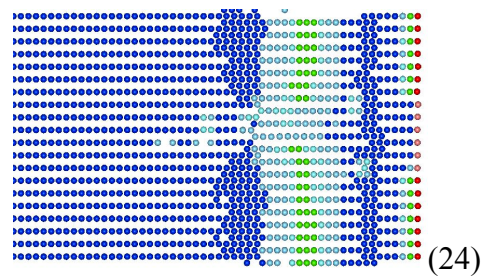
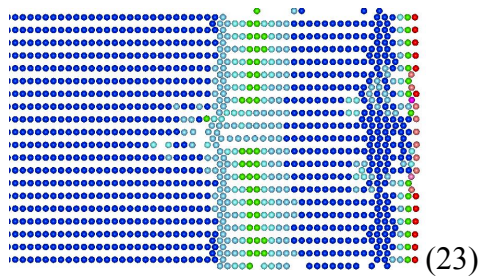
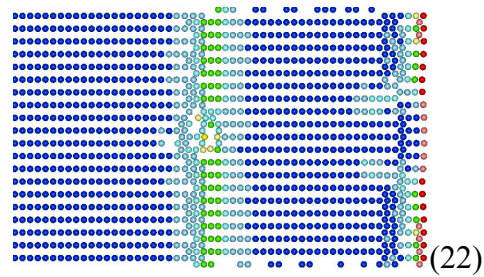
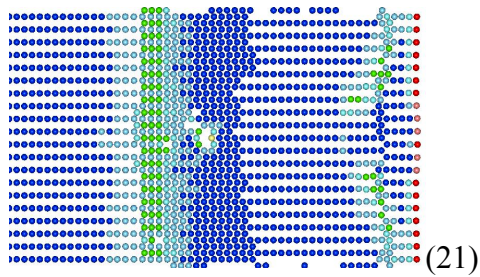
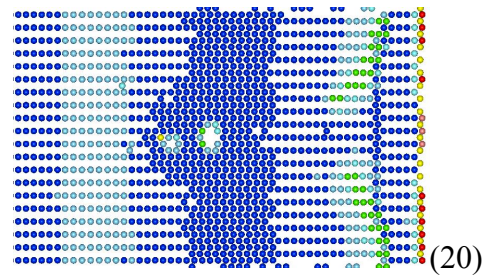
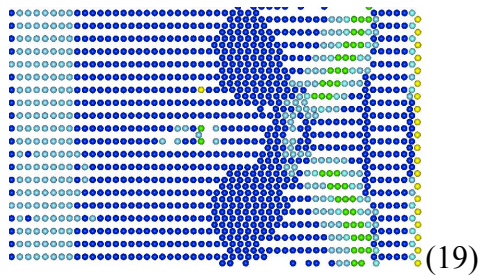
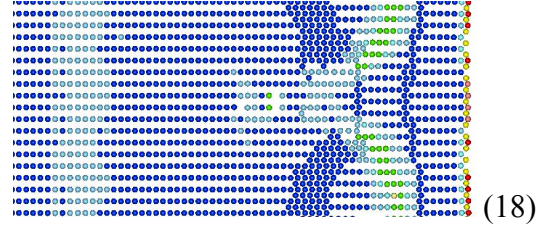
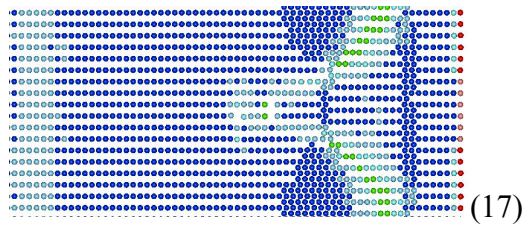
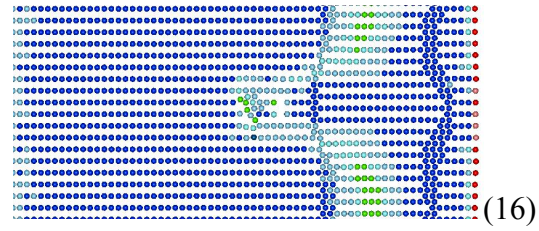
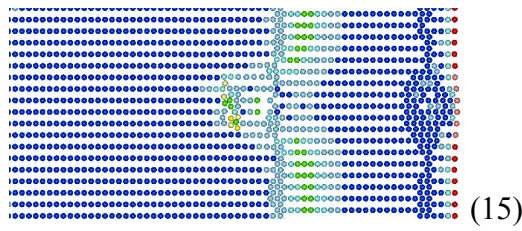


Figure 8. Snapshots of top views on the plane of  $y = 0$ .